Chinese Chemical Letters 33 (2022) 3573–3576

Contents lists available at ScienceDirect

Chinese Chemical Letters

journal homepage: www.elsevier.com/locate/cclet

Carbon dots and carbon nitride composite for photocatalytic removal of uranium under air atmosphere

Hongpeng Li[a,1], Qi Qing[a,1], Liyuan Zheng[b], Lan Xie[b], Zhiqiang Gan[b], Liqin Huang[a], Shuang Liu[a], Zhe Wang[b,*], Yuexiang Lu[a,*], Jing Chen[a]

[a] Institute of Nuclear and New Energy Technology, Tsinghua University, Beijing 100084, China
[b] The MOE Key Laboratory of Resources and Environmental System Optimization, College of Environmental Science and Engineering, North China Electric Power University, Beijing 102206, China

ARTICLE INFO

Article history:
Received 22 November 2021
Revised 16 January 2022
Accepted 18 January 2022
Available online 23 January 2022

Keywords:
Carbon dots
Carbon nitride
Uranium
Photocatalyst
Air atmosphere

ABSTRACT

Photocatalytic removal of uranium has attracted much attention in nuclear wastewater treatment and it is highly needed to develop functional photocatalyst with excellent removal performance. In this work, seven kinds of carbon dots/carbon nitride (CDs/CN) composites were synthesized and SerCDs/CN with the best photo-assisted uranium removal performance was screened out. It was found that the introduction of CDs could bring in higher photocurrent density, lower interfacial charge transfer impedance and narrower band gap, resulting in a much-improved removal performance. SerCDs/CN had shown a removal capacity as high as 1690 mg/g and the reaction could be operated under air atmosphere which is promising in real application.

Nuclear energy, with uranium as the main fuel, is a kind of promising energy due to its low greenhouse gas emission. The treatment of uranium-containing wastewater produced in the nuclear fuel cycle is important for both environment protection and fuel recycling. Adsorption has been proved to be an effective method for uranium removal from solution, and the adsorption capacity and reusability of the adsorbents are the key factors for improving the removal performance [1]. Recently, a photocatalysis-assisted adsorption strategy, in which uranium could be transformed from its soluble form to insoluble form, has been developed and could dramatically enhance the adsorption capacity [2]. Many photocatalyst have been synthesized for this method, such as TiO_2 [3–5], MOFs [6–8], modified graphene materials [9–11]. Among these materials, the metal-free carbon nitride has attracted much attention as it could be synthesized easily with low-cost, high stability, visible-light activity and would not introduce extra metal pollution to the solution [12,13]. While, the uranium removal performance of carbon nitride obtained from the traditional method is not good enough, thus many methods, such as element doping, surface modification and constructing composite, have been developed to improve the adsorption and photocatalytic performance [14–19].

Carbon dots (CDs) have shown great potential in many fields such as biosensing, biological imaging, drug delivery, optoelectronics, photovoltaic and photocatalysis due to their unique physical-chemical, optical and electronic properties. In particular, their excellent optical-induced electron transfer capabilities have attracted great interest from researchers for their application in photocatalytic fields [20–22]. Numerous works have been reported on the construction of g-C_3N_4/CDs composites and their applications in photocatalytic systems. By changing the raw material, synthesis methods and reaction conditions, the obtained heterogeneous g-C_3N_4/CDs nanocomposites could show broader absorption spectrum, appropriate electron band structure, faster carrier mobility, making them effective photocatalysts for different photocatalytic reactions [23–26]. However, the application of g-C_3N_4/CDs composites in photocatalytic uranium removal is rarely reported. It is attractive to develop and screening proper g-C_3N_4/CDs composites for this application.

In this work, seven kinds of CDs were synthesized and composited with g-C_3N_4. Compared to pure g-C_3N_4, the photo-assisted uranium removal performances of these seven composites were all increased due to the introduction of CDs. The morphological structure, photoelectric properties and photocatalytic uranium removal properties of the composites with best performance were system studied. It has shown an adsorption capacity of more than

* Corresponding authors.
E-mail addresses: wangzhe@ncepu.edu.cn (Z. Wang), luyuexiang@mail.tsinghua.edu.cn (Y. Lu).
[1] These two authors contributed equally to this work.

https://doi.org/10.1016/j.cclet.2022.01.050
1001-8417/

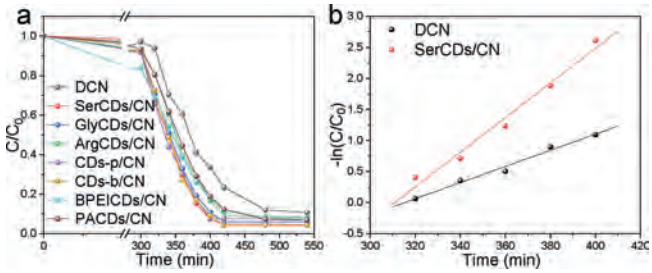

Fig. 1. (a) The photocatalytic performance of different CDs/CN composites for the elimination of uranium. (b) Photocatalytic rate fitting of DCN and SerCDs/CN.

1690 mg/g, and could work under air atmosphere, showing great application potential.

Seven kinds of carbon dots (CDs) were first synthesized by using different raw materials (Fig. S1 in Supporting information) [27–31]. All these CDs showed a typical fluorescence property of carbon dots, such as the emission peak shifted with the change of extinction wavelength (Fig. S2 in Supporting information), but with different emission peaks. The XRD and FTIR results also showed the difference of these CDs (Figs. S3 and S4 in Supporting information). Seven carbon dots/carbon nitride (CDs/CN) composites were then prepared by mixing corresponding CDs (1 wt%) with the dicyanamide precursor and heating at 500 °C for 4 h. The obtained CDs/CNs were named as ArgCDs/CN, BPEICDs/CN, GlyCDs/CN, CDs-p/CN, PACDs/CN, CDs-b/CN and SerCDs/CN. Carbon nitride prepared without adding CDs was named as DCN.

The XRD results showed that both the DCN and CDs/CN had characteristic diffraction peaks of the graphitic carbon nitride, indicating the presence of a layer structure (Fig. S3). FTIR suggested that the DCN and CDs/CN composites had the similar structural composition (Fig. S4). The emission wavelengths of all composites did not move with the excitation wavelength (Fig. S5 in Supporting information), so the composites did not present fluorescence properties of carbon dots, probably due to the low loading amount of carbon dots, of which the mass fraction only possessed 1 wt%. However, the fluorescence emission intensity of each composite varied with the excitation wavelength, and the profile and peak position of each composite varied, indicating that each carbon dot composite had its own properties.

The photocatalytic performances of different CDs/CN were carried out in Fig. 1. Before irradiated with visible light, CDs/CN was mixed with uranium solution in dark for 300 min to reach an adsorption equilibrium. During the light irradiation, each CDs/CN composite reached the maximum removal capacity for uranyl ion at around 180 min, while it was 540 min for DCN. The photocatalytic removal rate of SerCDs/CN was the highest all over the composites, which was 0.0279 min^{-1}, about two times of DCN (0.0130 min^{-1}). The removal rate of other catalysts was listed in Table S2 (Supporting information) and the photoreaction rates of each composite were fitted in Fig. S6 (Supporting information).

The morphological structure and photoelectric properties of SerCDs/CN were further studied to figure out the origin of the performance enhancement. As shown in Fig. 2a, the CDs were smaller than 10 nm and dispersed on the CNs nanosheets. The introduction of CDs could influence both the adsorption and photocatalytic property. The photo-current density of the SerCDs/CN composite was higher than DCN (Fig. 2b), which implied that electrons and holes could be separated more easily on the surface of SerCDs/CN under irradiation. The EIS spectra radius of SerCDs/CN was also smaller than DCN (Fig. 2c), suggesting that interfacial charge transfer impedance of the composite was smaller than pure DCN and the photogenerated charges could transfer more easily from the photo active site to the adsorption site

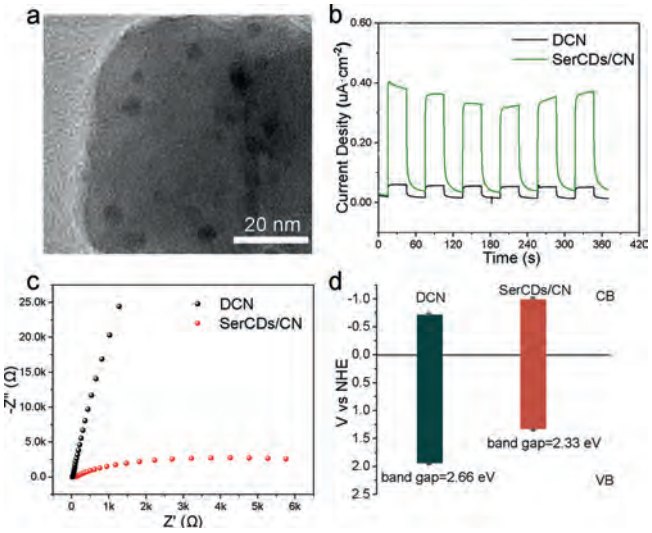

Fig. 2. (a) TEM image of SerCDs/CN. (b) Time dependent photocurrent responses under light irradiation, (c) EIS Nyquist plots and (d) illustration of energy level diagrams of DCN and SerCDs/CN composite.

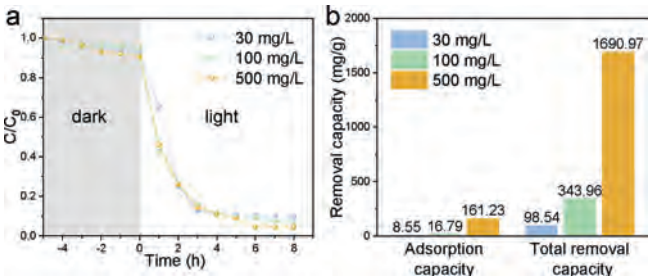

Fig. 3. (a) The photocatalytic performance and (b) the adsorption capacity in the dark condition and the total removal capacity after irradiation of SerCDs/CN with different concentration of uranium.

to react with uranium, improving the photocatalytic performance of the composite. The forbidden band width of the two carbon nitrides was acquired with solid UV–vis spectra, and Mott-Schottky curves were employed to obtain the conduction band value (Table S4 and Fig. S7 in Supporting information). As shown in Fig. 2d, the forbidden band width of SerCDs/CN was 2.33 eV, much less than DCN (2.66 eV), indicating it could utilize UV light as well as visible light below 532 nm, holding a higher utilization rate of light than DCN. These results indicated that the introduction of CDs could improve the photoelectric properties of CN.

The photocatalytic removal performance of SerCDs/CN was further investigated with different concentration of uranium (Fig. 3a). SerCDs/CN was mixed with uranium solution at dark condition for 300 min to reach an adsorption equilibrium and then irradiated with Xe lamp. The adsorption capacity and total removal capacity were listed in Fig. 3b and both were enhanced along with the increasing concentration of uranium. The final removal rate was all higher than 90% at different concentration. When the initial concentration of uranium was 500 mg/L, the adsorption capacity of SerCDs/CN was 161.2 mg/g and the removal rate after irradiating for 8 h could reach to 91% with an unsaturated removal capacity of 1690 mg/g.

To further understand the mechanism of the photo-assisted adsorption reaction, the final uranium products were collected and characterized with various methods. As show in Fig. 4a, the product on the surface of SerCDs/CN was rod-like, and the ESB mode scanning image in Fig. 4b verified the heavy metal elements were

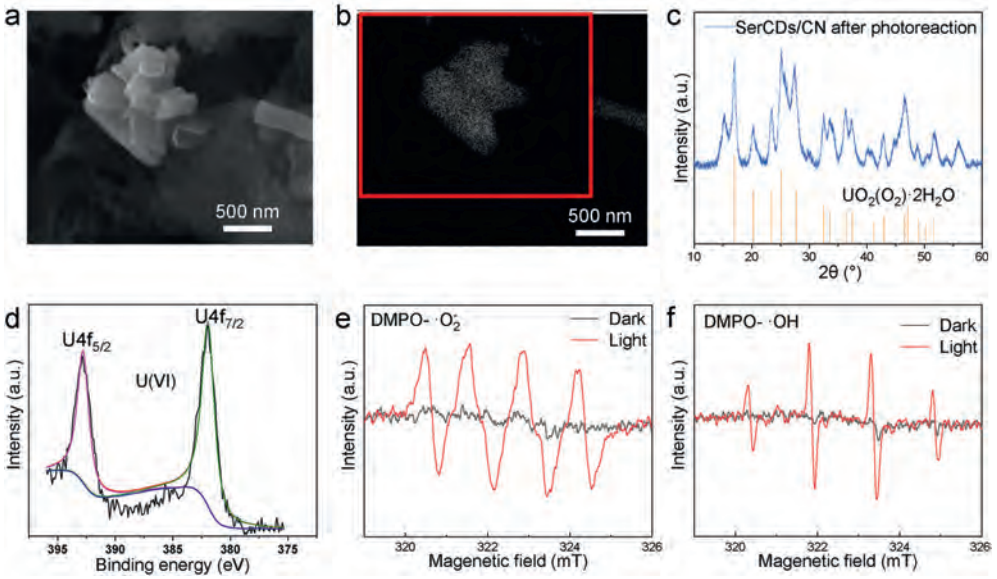

Fig. 4. (a) SEM image and (b) the ESB mode scanning image of SerCDs/CN after photocatalytic process. (c) The XRD pattern and (d) XPS spectra of the photocatalytic product. EPR signals of (e) DMPO-$^{\cdot}O_2^-$ spin adducts and (f) DMPO-$^{\cdot}$OH spin adducts generated in CH_3OH and H_2O system, respectively.

distributed on the rods. The EDX mapping results of this area in Fig. S8 (Supporting information) confirmed the existence of elements C, N, U and O. The XRD pattern (Fig. 4c) clearly showed that new diffraction peaks was obtained after photocatalytic reaction with uranium and the peaks were consistent with $UO_2(O_2)\cdot 2H_2O$ (PDF#35–0571). Besides, the valence state of uranium in the product was analyzed by XPS in Fig. 4d and the peaks were identified as U(VI), which also confirmed the products of uranium were mainly metastudtite.

In most of the previous reports on photo-induced adsorption method, it was proposed that soluble U(VI) could be reduced to insoluble U(IV) and deposited as UO_2 or other uranium oxide. While, in this work, it was found that the U(VI) was not reduced to U(IV) and the final product was not uranium oxide but uranium peroxide. The main difference of these two processes was that in the literature, the reaction was operated under inert gas, while in this work the reaction was operated under air atmosphere. The presence of oxygen might play an important role.

According to other report [32], the mechanism of photocatalytic reduction of uranyl ions to uranium dioxide in inert atmosphere such as nitrogen could be concluded in Eqs. 1-3:

$$UO_2^{2+} + e^- \rightarrow UO_2^{+} \quad (1)$$

$$UO_2^{+} + e^- \rightarrow UO_2(s) \quad (2a)$$

$$2UO_2^{+} \rightarrow UO_2^{2+} + UO_2(s) \quad (2b)$$

$$UO_2^{2+} + 2e^- \rightarrow UO_2(s) \quad (3)$$

Uranyl ion (UO_2^{2+}) could be reduced to $UO_2(s)$ in multiple ways: Firstly, uranyl ion could be reduced to U(V) by a single photoelectron (Eq. 1). Then UO_2^{+} could be further reduced by a single photoelectron to UO_2 (Eq. 2a) or generate UO_2^{2+} and UO_2 through the disproportionation (Eq. 2b). It was also possible that UO_2^{2+} could be reduced to UO_2 directly with a one-step two-electron reduction pathway (Eq. 3).

In this work, due to the generation of metastudtite, it could be speculated that hydrogen peroxide was produced under light irradiation, and it could react with uranyl ion or uranium dioxide to produce metastudtite. The possible reaction paths were listed as Eqs. 4–12.

$$g\text{-}C_3N_4 + h\nu \rightarrow h^+ + e^- \quad (4)$$

$$O_2 + 2H^+ + 2e^- \rightarrow H_2O_2 \ (0.68\ V\ vs.\ NHE) \quad (5)$$

$$O_2 + e^- \rightarrow \cdot O_2^- (-0.16\ V\ vs.\ NHE) \quad (6)$$

$$\cdot O_2^- + e^- + 2H^+ \rightarrow H_2O_2 (1.44\ V\ vs.\ NHE) \quad (7)$$

$$\cdot O_2^- + H_2O_2 \rightarrow \cdot OH + OH^- + O_2 \quad (8)$$

$$CH_3OH + \cdot OH/\cdot O_2^- \rightarrow CO_2 + H_2O \quad (9)$$

$$UO_2^{2+} + H_2O_2 + 2H_2O \rightarrow UO_2(O_2)\cdot 2H_2O + 2H^+ \quad (10)$$

$$UO_2^{2+} + 2e^- \rightarrow UO_2 \quad (11)$$

$$UO_2 + O_2 + 4H_2O \rightarrow UO_2(O_2)\cdot 2H_2O \quad (12)$$

H_2O_2 could be generated through two pathways. The first one was that oxygen was reduced to H_2O_2 directly by two photoelectrons (Eq. 5). The other one was that oxygen was first reduced to $\cdot O_2^-$ by one photoelectron (Eq. 6) and then $\cdot O_2^-$ was reduced to H_2O_2 by another photoelectron (Eq. 7). The EPR spectra in the absence of uranium were carried out to investigate the photocatalytic products with SerCDs/CN under irradiation.

As exhibited in Figs. 4e and f, the yield of both $\cdot O_2^-$ and $\cdot$OH increased significantly under the light irritation, indicating the existence of reactions in Eqs. 6-8. In detail, SerCDs/CN could reduce O_2 to $\cdot O_2^-$ because the CB of the catalyst was more negative than the redox potential of $\cdot O_2^-/O_2$ (−0.16 eV). As a result, in this work, the oxygen was reduced to H_2O_2 *via* a two-step reduction with $\cdot O_2^-$ as the intermediate products. Then H_2O_2 could react with UO_2^{2+} to form $UO_2(O_2)\cdot 2H_2O$ (Eq. 10). It was also possible that the UO_2^{2+} was first reduced to UO_2 (Eq. 11) and then react with

oxygen to form $UO_2(O_2)•2H_2O$ (Eq. 12). The current experiment results could not verify the existence of this reaction, which should be investigated in future research. Based on the above theory, other photocatalysts that could produce H_2O_2 could also be used for this mechanism.

In summary, we have synthesized seven kinds of carbon dots/carbon nitride composites and SerCDs/CN with the best photo-assisted uranium removal performance was screened out. It was found that the introduction of CDs to CNs, could result in higher photocurrent density, lower interfacial charge transfer impedance and narrower band gap. SerCDs/CN had shown a removal capacity as high as 1690 mg/g and most importantly the reaction could be operated under air atmosphere which is more promising in real application than that operated under inert gas. The final product was found to be $UO_2(O_2)•2H_2O$, which was different with most of other reports. Our work has further proved that the photo-induced extraction of uranium could be operated under air atmosphere. This work and further study of the formation mechanism of $UO_2(O_2)•2H_2O$ would open a new way for the photocatalytic removal of uranium, and more photocatalysts could be designed and synthesized for this application.

Declaration of competing interest

The authors declare that they have no known competing financial interests or personal relationships that could have appeared to influence the work reported in this paper.

Acknowledgments

We would like to acknowledge the National Natural Science Foundation of China (Nos. 21976104, 21906051) and the Fundamental Research Funds for the Central Universities (No. 2019MS046). LingChuang Research Project of China National Nuclear Corporation is also gratefully acknowledged.

Supplementary materials

Supplementary material associated with this article can be found, in the online version, at doi:10.1016/j.cclet.2022.01.050.

References

[1] B.M. Jun, H.K. Lee, T. Kim, Sep. Purif. Technol. 278 (2021) 119675.
[2] V. Kumar, V. Singh, K.H. Kim, E. Kwon, S. Younis, Coord. Chem. Rev. 447 (2021) 214148.
[3] P. Li, J. Wang, Y. Wang, et al., Chem. Eng. J. 365 (2019) 231–241.
[4] J. Yu, C. Yu, W. Zhu, et al., Chemosphere 286 (2022) 131626.
[5] X. Gong, L. Tang, J. Zou, et al., J. Hazard. Mater. 423 (2022) 126935.
[6] H. Li, F. Zhai, D. Gui, et al., Appl. Catal. B: Environ. 254 (2019) 47–54.
[7] H. Zhang, W. Liu, A. Li, et al., Angew. Chem. Int. Ed. 58 (2019) 16110–16114.
[8] H. Gao, J. Xu, J. Zhou, S. Zhang, R. Zhou, J. Colloid. Interf. Sci. 570 (2020) 125–134.
[9] Z. Dai, Y. Sun, H. Zhang, D. Ding, L. Li, Chemosphere 254 (2020) 126671.
[10] Z. Dong, Z. Zhang, Z. Li, et al., Environ. Sci. Nano 8 (2021) 2372–2385.
[11] Z. Wang, H. Liu, Z. Lei, et al., Chem. Eng. J. 402 (2020) 126256.
[12] Y. Xing, X. Wang, S. Hao, et al., Chin. Chem. Lett. 32 (2021) 13–20.
[13] W. Zhang, L. Li, Y. Gao, D. Zhang, New J. Chem. 44 (2020) 19961–19976.
[14] X. Bai, L. Wang, Y. Wang, W. Yao, Y. Zhu, Appl. Catal. B: Environ. 152 (2014) 262–270.
[15] W. Zhang, Z. Zhang, S. Kwon, et al., Appl. Catal. B: Environ. 206 (2017) 271–281.
[16] S. Liu, Z. Wang, Y. Lu, et al., Appl. Catal. B: Environ. 282 (2021) 119523.
[17] L. Jiang, Y. Xie, F. He, et al., Chin. Chem. Lett. 32 (2021) 2187–2191.
[18] B. Li, L.C. Nengzi, R. Guo, et al., Chin. Chem. Lett. 31 (2020) 2705–2711.
[19] H. Li, Z. Wang, Y. Lu, et al., Appl. Surf. Sci. 531 (2020) 147307.
[20] C. He, P. Xu, X. Zhang, W. Long, Carbon 186 (2021) 91–127.
[21] X. Zhang, X. Liao, Y. Hou, et al., J. Hazard. Mater. 422 (2021) 126881.
[22] Z. Wang, L. Zhang, K. Zhang, et al., Chemosphere 287 (2021) 132313.
[23] X. Miao, X. Yue, Z. Ji, et al., Appl. Catal. B: Environ. 227 (2018) 459–469.
[24] Z. Xie, Y. Feng, F. Wang, et al., Appl. Catal. B: Environ. 229 (2018) 96–104.
[25] Y. Nie, F. Yu, L. Wang, et al., Appl. Catal. B: Environ. 227 (2018) 312–321.
[26] Y. Jiao, Q. Huang, J. Wang, Z. He, Z. Li, Appl. Catal. B: Environ. 247 (2019) 124–132.
[27] Y. Dong, R. Wang, H. Li, et al., Carbon 50 (2012) 2810–2815.
[28] W. Wang, Y. Lu, H. Huang, et al., Biosens. Bioelectron. 64 (2015) 517–522.
[29] H. Ding, S. Yu, J. Wei, H. Xiong, ACS Nano 10 (2016) 484–491.
[30] Z. Wang, Y. Xie, Z. Lei, et al., Anal. Chem. 91 (2019) 9690–9697.
[31] Z. Wang, C. Xu, Y. Lu, et al., Sensor. Actuat. B: Chem. 241 (2017) 1324–1330.
[32] P. Li, J. Wang, Y. Wang, et al., J. Photochem. Photobiol. C: Photochem. Rev. 41 (2019) 100320.